VOLUME 117, NUMBER 27
JULY 12, 1995

JOURNAL OF THE AMERICAN CHEMICAL SOCIETY

Anti-Metallocene Antibodies: A New Approach to Enantioselective Catalysis of the Diels–Alder Reaction‡

Jari T. Yli-Kauhaluoma,† Jon A. Ashley, Chih-Hung Lo, Lee Tucker, Mary M. Wolfe, and Kim D. Janda*

Contribution from the Departments of Molecular Biology and Chemistry, The Scripps Research Institute, 10666 North Torrey Pines Road, La Jolla, California 92037

Received February 1, 1995®

Abstract: We have shown how a constrained bicyclo[2.2.2]octene hapten can elicit antibody catalysts for the Diels–Alder reaction between 4-carboxybenzyl *trans*-1,3-butadiene-1-carbamate and *N,N*-dimethylacrylamide (Gouverneur, V. E.; de Pascual-Teresa, B.; Beno, B.; Janda, K. D.; Lerner, R. A. *Science* **1993**, *262*, 204). In the present study we have developed a new approach to hapten design for elicitation of Diels–Alder catalytic antibodies. Our strategy was to engage the freely rotating η^5-cyclopentadienyl iron complex as the haptenic group. By applying such a flexible hapten we set out to determine if the immune system could freeze out a conformer which mimics the Diels–Alder transition state and hence produce new Diels–Alderases. If so, how would the catalytic rates, diastereo- and enantioselectivity of these antibodies compare with those of antibodies elicited by the former methodology? We generated antibodies that catalyzed the Diels–Alder reaction with high enantio- and diastereoselectivity and had effective molarities (EM) comparable to those of antibodies elicited using the constrained bicyclo[2.2.2]octene haptens. This methodology offers a new approach to the production of antibodies for the catalysis of other reactions with pericyclic, highly-ordered transition states.

Introduction

In view of its synthetic utility and the lack of a known biological catalyst, the Diels–Alder reaction has been seen as an important focus for the catalytic antibody field.[1-3] A number of groups, including our own, have successfully generated antibodies capable of catalyzing Diels–Alder cycloaddition reactions.[4,5] Our initial approach, using the bicyclo[2.2.2]octene haptens **1** and **2** (Figure 1), was to induce antibody catalysts which could individually control the product distribution of the reaction between diene **3** and dienophile **4**.[6] The selection of these highly constrained structures (**1** and **2**) was based on elegant work previously reported by Schultz,[4b] who hypothesized that the bicyclo[2.2.2]octene system might be a good mimic for the ordered transition state of the Diels–Alder reaction. This was later confirmed by *ab initio* calculations.[5]

* Author to whom correspondence should be addressed.
† On leave from The Technical Research Centre of Finland, Chemical Technology, Biologinkuja 7, FIN-02150 Espoo, Finland.

‡ Abbreviations: EDIA, *N,N*-diisopropylethylamine; TEA, triethylamine; *t*-BOC, *tert*-butoxycarbonyl; BOPCl, bis(2-oxo-3-oxazolidinyl)phosphinic chloride; 3-NBA, 3-nitrobenzyl alcohol; PMA, phosphomolybdic acid; DSS, sodium 2.2-dimethyl-2-silapentan-5-sulfonate; EDC, 1-(3-dimethylaminopropyl)-3-ethylcarbodiimide hydrochloride.

® Abstract published in *Advance ACS Abstracts*, June 15, 1995.

(1) (a) Diels, O.; Alder, K. *Liebigs Ann. Chem.* **1928**, *460*, 98–122. (b) Carruthers, W. *Cycloaddition Reactions in Organic Chemistry*; Tetrahedron Organic Chemistry Series Volume 8; Pergamon Press: Oxford, 1990. (c) Oppolzer, W. Intermolecular Diels–Alder reactions. In *Comprehensive Organic Synthesis*; Trost, B. M., Fleming, I., Paquette, L. A., Eds.; Pergamon Press: Oxford, 1991; Vol. 5, pp 315–399. (d) Oppolzer, W. *Angew. Chem., Int. Ed. Engl.* **1977**, *16*, 10–23. (e) Pindur, U.; Lutz, G.; Otto, C. *Chem. Rev.* **1993**, *93*, 741–761. (f) Oppolzer, W. *Angew. Chem., Int. Ed. Engl.* **1984**, *23*, 876–889. (g) Kagan, H. B.; Riant, O. *Chem. Rev.* **1992**, *92*, 1007–1019. (h) Narasaka, K. *Synthesis* **1991**, 1–11.

(2) For biocatalytic methods in the Diels–Alder reactions, see for example: (a) Colonna, S.; Manfredi, A.; Annunziata, R. *Tetrahedron Lett.* **1988**, *29*, 3347–3350. (b) Rama Rao, K.; Srinivasan, T. N.; Bhanumathi, N. *Tetrahedron Lett.* **1990**, *31*, 5959–5960. The use of bovine serum albumin and baker's yeast to catalyze the Diels–Alder reaction is reported in these communications, respectively.

0002-7863/95/1517-7041$09.00/0

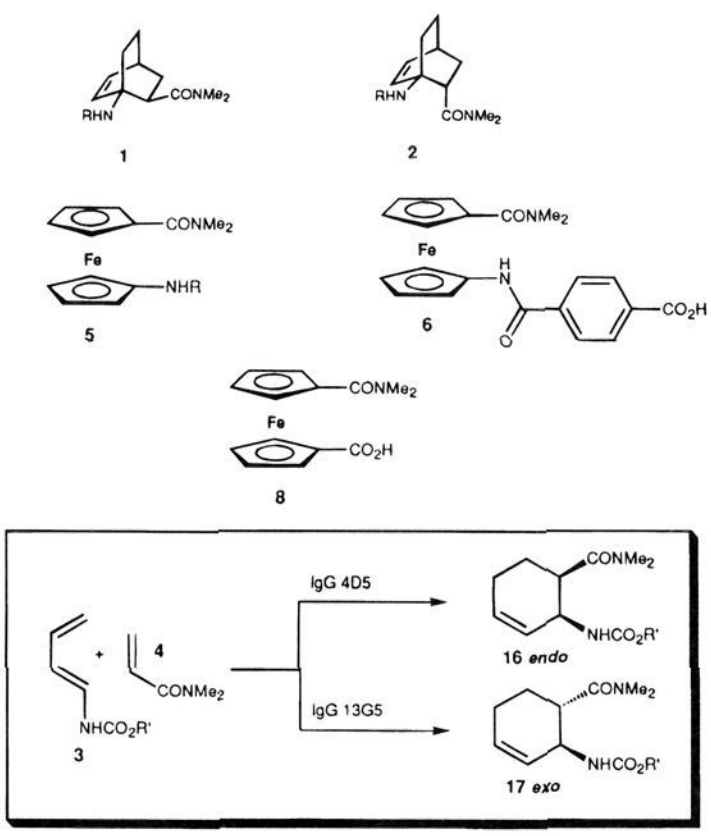

Figure 1. Antibody-catalyzed Diels–Alder reactions and the structures of haptens **1**, **2**, **5**, and **6** and inhibitor **8** used in the present study. R = $CO(CH_2)_3CO_2H$, R′ = 4-carboxybenzyl.

In our new strategy, we intended to challenge the notion that the best haptens for reactions proceeding through highly ordered transition states must be conformationally restricted analogs. Rather, we wondered how the immune system would "recognize" a conformationally unrestricted hapten. We were interested in using the dicyclopentadienyl system of ferrocene as a loose mimic for the cyclic, six-membered transition state of the Diels–Alder reaction. Clearly, from the vast immune library, antibodies to all stable conformers of the molecule should exist. However, critical to our success would be antibody recognition and the freezing out of a conformer which resembled the Diels–Alder transition state. Therefore, this conformationally flexible haptenic design offered an interesting, antithetical approach to antibody-catalysis of the Diels–Alder reaction.

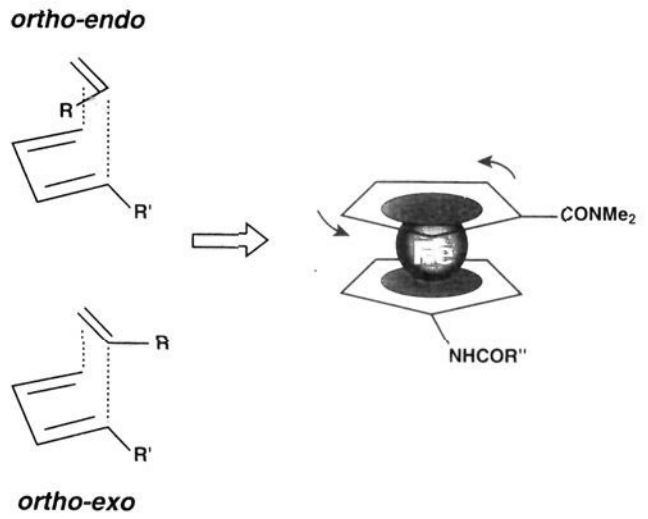

Figure 2. Representations of the transition states for the *ortho-endo* and *ortho-exo* Diels–Alder reactions and the corresponding ferrocene structure for these transition states. R = $CONMe_2$, R′ = $NHCO_2$-$CH_2(C_6H_4)CO_2H$, R″ = $(CH_2)_3CO_2H$ or 4-carboxyphenyl.

Results and Discussion

The decision to utilize ferrocene complexes **5** and **6** as haptens was threefold in nature. First, these haptens have two pentagonal, delocalized, π-electron ring systems stacked upon each other, in a sandwich-type arrangement, with an inter-ring distance of ≈3.3 Å.[7] Such a network would not only be highly immunogenic but might also elicit antibodies with combining sites which could guide the diene and dienophile into a reactive, ternary complex. Second, exploitation of rotational freedom was pivotal in this hapten design. The barrier of rotation around the common axis in this type of cyclopentadienyl metal complex is low (≈2–5 kcal mol^{-1}).[7,8] Hence, the rotation of the rings with respect to each other should not be restricted. This feature provides an opportunity to mimic the diastereomeric transition states of the Diels–Alder reaction and the exciting possibility of generating, with a single hapten, antibodies that could catalyze the formation of all diastereomers (Figure 2). Third, the lipophilic character inherent in the disubstituted η^5-cyclopentadienyl system of haptens **5** and **6** should induce a hydrophobic microenvironment in the antibody's combining site. This should serve to enhance sequestering of the diene and dienophile from aqueous solution and improve observed rates.

Hapten and Substrate Synthesis. Hapten **5** was prepared in the following manner. Amide bond formation was accomplished between 1,1′-ferrocenedicarboxylic acid **7** and dimethylamine hydrochloride using bis(2-oxo-3-oxazolidinyl)-

(3) There is some indirect experimental evidence for a biological Diels–Alder reaction involving diene and dienophile precursors in the biosynthesis of solanapyrones although the isolation and characterization of a natural Diels–Alderase is yet to be described: (a) Oikawa, H.; Suzuki, Y.; Naga, A.; Katayama, K.; Ichihara, A. *J. Am. Chem. Soc.* **1994**, *116*, 3605–3606. (b) Oikawa, H.; Yokota, T.; Abe, T.; Ichihara, A.; Sakamura, S.; Yoshizawa, Y.; Vederas, J. C. *J. Chem. Soc., Chem. Commun.* **1989**, 1282–1284. (c) Oikawa, H.; Yokota, T.; Ichihara, A.; Sakamura, S. *J. Chem. Soc., Chem. Commun.* **1989**, 1284–1285. For several examples of postulated biosynthetic Diels–Alder adducts, see for example: (a) Sanz-Cervera, J. F.; Glinka, T.; Williams, R. M. *J. Am. Chem. Soc.* **1993**, *115*, 347–348, and references cited therein. (b) Stipanovic, R. D. *Environ. Sci. Res.* **1992**, *44*, 319–328, and references cited therein. (c) Cane, D. E.; Tan, W.; Ott, W. R. *J. Am. Chem. Soc.* **1993**, *115*, 527–535. (d) Hano, Y.; Ayukawa, A.; Nomura, T. *Naturwissenschaften* **1992**, *79*, 180–182. (e) Ikuta, J.; Fukai, T.; Nomura, T.; Ueda, S. *Chem. Pharm. Bull.* **1986**, *34*, 2471–2478. (f) Takasugi, M.; Nagao, S.; Masamune, T.; Shirata, A.; Takahashi, K. *Chem. Lett.* **1980**, 1573–1576. (g) Bell, A. A.; Stipanovic, R. D.; O'Brien, D. H.; Fryxell, P. A. *Phytochemistry* **1978**, *17*, 1297–1305. (h) Ueda, S.; Nomura, T.; Fukai, T.; Matsumoto, J. *Chem. Pharm. Bull.* **1982**, *30*, 3042–3045. (i) Hano, Y.; Aida, M.; Nomura, T.; Ueda, S. *J. Chem. Soc., Chem. Commun.* **1992**, 1177–1178. (j) Oikawa, H.; Murakami, Y.; Ichihara, A. *J. Chem. Soc., Perkin Trans. 1* **1992**, 2955–2959.

(4) (a) Hilvert, D.; Hill, K. W.; Nared, K. D.; Auditor, M.-T. M. *J. Am. Chem. Soc.* **1989**, *111*, 9261–9262. (b) Braisted, A. C.; Schultz, P. G. *J. Am. Chem. Soc.* **1990**, *112*, 7430–7431. (c) Suckling, C. J.; Tedford, M. C.; Bence, L. M.; Irvine, J. I.; Stimson, W. H. *Bioorg. Med. Chem. Lett.* **1992**, *2*, 49–52. (d) Suckling, C. J.; Tedford, M. C.; Bence, L. M.; Irvine, J. I.; Stimson, W. H. *J. Chem. Soc., Perkin Trans. 1* **1993**, 1925–1929.

(5) Gouverneur, V. E.; de Pascual-Teresa, B.; Beno, B.; Janda, K. D.; Lerner, R. A. *Science* **1993**, *262*, 204–208.

(6) Our choice of using *trans*-1-*N*-carbamoylamino-1,3-butadiene and *N*,*N*-dimethylacrylamide as reactants can be traced to the numerous synthetic routes in which they are employed. Oppolzer and co-workers have exploited *N*-acyl-*N*-alkyl-1-amino-1,3-dienes in the intramolecular Diels–Alder reaction to synthesize natural products, *e.g.*, (−)-pumiliotoxin-C. (a) Oppolzer, W.; Fröstl, W. *Helv. Chim. Acta* **1977**, *58*, 590–593. (b) Oppolzer, W.; Fröstl, W.; Weber, H. P. *Helv. Chim. Acta* **1975**, *58*, 593–595. (c) Oppolzer, W.; Flaskamp, E. *Helv. Chim. Acta* **1977**, *60*, 204–207. (d) Oppolzer, W.; Fröstl, W. *Helv. Chim. Acta* **1975**, *58*, 587–589. Overman and co-workers have used *N*-acyl-1-amino-1,3-dienes in intermolecular Diels–Alder reactions to solve stereochemical problems in the synthesis of the alkaloids (±)-pumiliotoxin-C and (±)-gephyrotoxin. (e) Overman, L. E.; Lesuisse, D.; Hashimoto, M. *J. Am. Chem. Soc.* **1983**, *105*, 5373–5379. (f) Overman, L. E.; Fukaya, C. *J. Am. Chem. Soc.* **1980**, *102*, 1454–1456. (g) Overman, L. E.; Jessup, P. J. *Tetrahedron Lett.* **1977**, *14*, 1253–1256. (h) Overman, L. E.; Jessup, P. E. *J. Am. Chem. Soc.* **1978**, *100*, 5179–5185. In addition, Danishefsky has reported the synthesis of the unnatural amino acid isogabaculine. (i) Danishefsky, S.; Hershenson, F. M. *J. Org. Chem.* **1979**, *44*, 1180–1181.

(7) (a) Rosenblum, M. *Chemistry of the Iron Group Metallocenes*; John Wiley & Sons: New York, 1965; pp 29–61. (b) Deeming, A. J. Mononuclear Iron Compounds with η^2–η^6 Hydrocarbon Ligands; In *Comprehensive Organometallic Chemistry*; Wilkinson, G., Stone, F. G. A., Abel, E. W., Eds.; Pergamon Press: Oxford, 1982; Vol. 4; pp 377–512.

Scheme 1. Preparation of Haptens **5** and **6**[a]

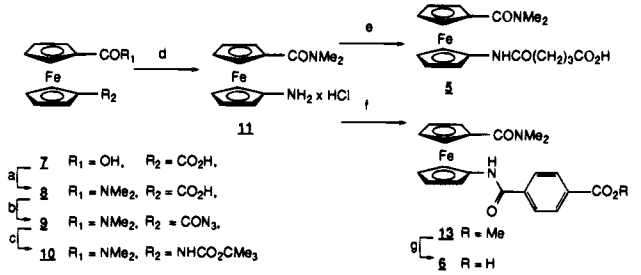

[a] (a) $Me_2NH{\cdot}HCl$, BOPCl, EDIA, $CHCl_3$, 0 °C, 1 h, 58%; (b) $(PhO)_2PON_3$, TEA, PhMe, room temperature, 25 min, 98%; (c) *t*-BuOH, PhH, Δ, 15 min, 83%; (d) 4 M HCl in 1,4-dioxane, room temperature, 20 min, 85%; (e) glutaric anhydride, EDIA, $CHCl_3$, 0 °C, 89%; (f) **12**, EDIA, $CHCl_3$, 0 °C, 13 h, 90%; (g) $LiOH{\cdot}H_2O$, $MeOH/H_2O$ (5:1), 0 °C, 25 min, 91%.

phosphinic chloride[9] as the coupling agent (7.0 equiv of EDIA, $CHCl_3$, 0 °C, 1 h). Using this type of coupling reaction, monoamide **8** was obtained in a moderate yield of 58%. A modified Curtius rearrangement of the acyl azide **9** prepared from **8**, with diphenylphosphoryl azide (2 equiv of TEA, PhMe, room temperature, 25 min, 98%) gave the *tert*-butyl carbamate **10** (*t*-BuOH, PhH, 95 °C, 15 min, 83%).[10,11] Hapten **5** with a glutaryl linker was obtained in a 76% yield (two steps) from **10** after removal of the *tert*-butoxycarbonyl group and reaction with glutaric anhydride in the presence of *N,N*-diisopropylethylamine in chloroform (Scheme 1).

Hapten **6** was synthesized by coupling ferrocenyl amine **11** and methyl 4-chloroformylbenzoate **12** (EDIA, $CHCl_3$, 0 °C, 13 h, 90%). The hydrolysis of methyl ester **13** provided hapten **6** with a phenyl linker ($LiOH{\cdot}H_2O$, $MeOH/H_2O$ 5:1, 0 °C, 25 min, 91%) (Scheme 1).

The substrate diene, 4-carboxybenzyl *trans*-1,3-butadiene-1-carbamate **3**, was prepared from *trans*-2,4-pentadienoic acid **14** in four steps with minor modifications of the work reported by the Weinstock and Overman groups.[12] Briefly, formation of a mixed anhydride and acyl azide was followed by Curtius rearrangement in the presence of methyl 4-(hydroxymethyl)-benzoate (Scheme 2). The methyl ester of carbamate **15** was hydrolyzed to afford the diene substrate **3**. This was converted to its sodium salt by neutralizing the suspension of the carboxylic acid in 10 mM PBS, with an equivalent of NaOH.

Hybridoma Generation. Haptens **5** and **6** were conjugated to the carrier proteins keyhole limpet hemocyanin (KLH) and bovine serum albumin (BSA).[13] Conjugation was performed in the absence of ambient light as aqueous solutions of **5** and **6** are highly prone to photooxidation.

Scheme 2. Preparation of Diene Substrate **3**[a]

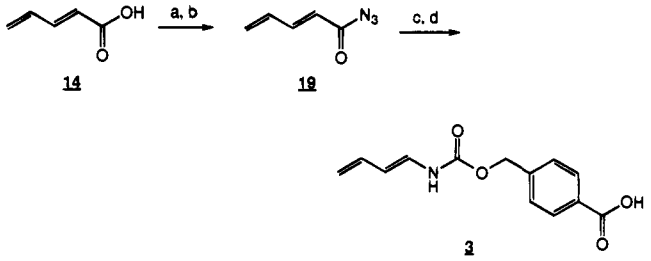

[a] (a) EtO_2CCl, EDIA, acetone, 0 °C, 1 h; (b) NaN_3 in H_2O, 0 °C, 45 min; (c) methyl 4-(hydroxymethyl)benzoate, PhMe, 100 °C, 40 min, 51%; (d) $LiOH{\cdot}H_2O$, $MeOH/H_2O$ (20:1), 0 °C, 90 min, 87%.

Following hyperimmunization of 129GIX$^+$ mice with the KLH conjugates of haptens **5** and **6**, monoclonal antibodies were elicited using hybridoma techniques.[14] Thus, female 129GIX$^+$ mice were injected *intraperitoneally* (ip) with KLH-**5** and KLH-**6** emulsified in RIBI (MPL/TDM) adjuvant. After three rounds of immunization with both haptenic conjugates and RIBI (MPL/TDM) adjuvant, mice were hyperimmunized with KLH-**5** and KLH-**6** in the absence of adjuvant. Fusions were performed after 3 days. The splenocytes were fused with the SP2/0 myeloma cell line, and BSA-**5** and BSA-**6** were used in the screening of hybridoma cell supernatants in an enzyme-linked immunosorbent assay (ELISA).[15] Because of the sensitivity of **5** and **6** to light, the ELISAs were carried out in the dark. A total of 33 and 38 hybridoma cell lines were found to be secreting monoclonal antibodies specific for BSA-**5** and BSA-**6**, respectively. All antibodies were of the IgG isotype and were purified by a process of ammonium sulfate precipitation, anion-exchange chromatography (DEAE), and affinity chromatography (protein G). Antibodies were judged to be >95% homogeneous by sodium dodecyl sulfate polyacrylamide gel electrophoresis (SDS-Page).[16]

Kinetic Analysis. Initial rates of the cycloaddition reaction between **3** and **4** were assayed in the absence and presence of antibody at 37 °C in 10 mM phosphate buffered saline (PBS), pH 7.4. The formation of the *ortho* Diels–Alder adducts **16** and **17** was monitored by reverse-phase HPLC under conditions which allowed separation of the *exo* and *endo* diastereomers.[17] Using these conditions, seven antibodies were found to be catalysts when the pool of antibodies specific to BSA-**5** were screened (1 *endo*, 6 *exo*). The KLH conjugate of **6** elicited eight antibody catalysts from the pool tested (7 *endo*, 1 *exo*). From these catalytic antibody subsets the most efficient *endo* (4D5, BSA-**6**) and *exo* (13G5, BSA-**5**) catalysts were chosen for further studies.

The kinetics of both antibody-catalyzed reactions were determined by measuring the differences in initial rates between the catalyzed and uncatalyzed reactions. Initial velocities were determined by following the formation of *endo* and *exo* adducts (<10% reaction completed). Catalysis of both the *endo* and

(8) Electron diffraction studies of ferrocene in the gas phase, ^{13}C NMR relaxation studies, neutron incoherent quasi-elastic scattering studies, dielectric measurements, and dynamic NMR studies of the 1,1′-disubstituted ferrocenes have provided evidence for the absence of an appreciable barrier of rotation of the rings about the common rotational axis. Moreover, X-ray data suggest that in the crystalline state considerable torsional vibration of the rings may persist. (a) Siebold, E. A.; Sutton, L. E. *J. Chem. Phys.* **1955**, *23*, 1967. (b) Mann, B. E.; Spencer, C. M.; Taylor, B. F. *J. Chem. Soc., Dalton Trans.* **1984**, 2027–2028. (c) Levy, G. L. *Tetrahedron Lett.* **1972**, 3709–3712. (d) Gardener, A. B.; Howard, J.; Waddington. T. C. *Chem. Phys.* **1981**, *57*, 453–460. (e) Sorriso, S. *J. Organomet. Chem.* **1979**, *179*, 205–213. (f) Jakusek, E.; Kolodziej, H. A.; Rozpenk, M.; Sorriso, S. *J. Mol. Struct.* **1982**, *79*, 341–344. (g) Abel, E. W.; Long, N. J.; Orrell, K. G.; Osborne, A. G.; Sik, V. *J. Organomet. Chem.* **1991**, *403*, 195–208. (h) Dunitz, J. D.; Orgel, L. E.; Rich, A. *Acta Crystallogr.* **1956**, *9*, 373.

(9) Diago-Meseguer, J.; Palomo-Coll, A. L.; Fernandez-Lizarbe, J. R.; Zugara-Bilbao, A. *Synthesis* **1980**, 547–551.

(10) Shioiri, T.; Ninomiya, K.; Yamada, S. *J. Am. Chem. Soc.* **1972**, *94*, 6203–6205.

(11) Patel, D. V.; Rielly-Gauvin, K.; Ryono, D. E.; Free, C. A.; Smith, S. A.; Petrillo, E. W. *J. Med. Chem.* **1993**, *36*, 2431–2447.

(12) (a) Weinstock, J. *J. Org. Chem.* **1961**, *26*, 3511. (b) Overman, L. E.; Taylor, G. F.; Petty, C. B.; Jessup, P. J. *J. Org. Chem.* **1978**, *43*, 2164–2167. (c) Jessup, P. J.; Petty, B.; Roos, J.; Overman, L. E. *Organic Syntheses*; Wiley: New York, 1988; Collect. Vol. 6, pp 95–101.

(13) (a) Staros, J. V.; Wright, R. W.; Swingle, D. M. *Anal. Biochem.* **1986**, *156*, 220. (b) Staros, J. V. *Biochemistry* **1982**, *21*, 3950. (c) Anjaneyulu, P. S. R.; Staros, J. V. *Int. J. Pept. Protein Res.* **1987**, *30*, 117.

(14) (a) Harlow, E.; Lane, D. *Antibodies: A Laboratory Manual*; Cold Spring Harbor Laboratory: New York, 1988. (b) Köhler, G.; Milstein, C. *Nature (London)* **1975**, *256*, 495. (c) Goding, J. W. *Monoclonal Antibodies: Principles and Practice*; Academic Press: San Diego, 1986.

(15) Engvall, E. *Methods Enzymol.* **1980**, *70*, 419.

(16) Laemmli, V. *Nature (London)* **1970**, *227*, 680–685.

(17) Formation of the *meta* regioisomers was not detected in any of our antibody-catalyzed or background reaction mixtures by either HPLC or ^1H-NMR.

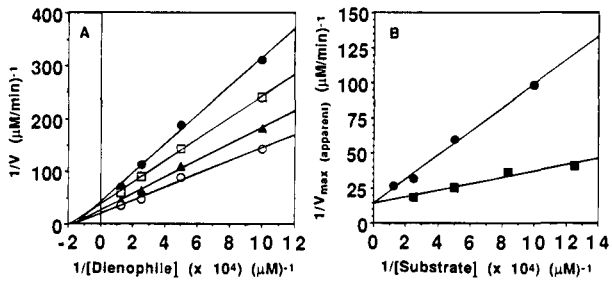

Figure 3. (A) Double reciprocal plot of initial velocities of *endo* adduct **16** formation in the presence of 4D5. Diene **3** concentrations were fixed (●, 0.8 mM; □, 1.2 mM; ▲, 2.0 mM; and ○, 4.0 mM), while dienophile concentrations varied from 1 to 8 mM. For the *exo* 13G5 assays seven fixed diene concentrations from 0.67 to 8 mM and the same four dienophile concentrations were used. (B) Replot of the apparent V_{max} values from the Lineweaver–Burk plots versus substrate concentrations (●, dienophile and ■, diene) to obtain the true V_{max} value as $1/(y$ intercept) and Michaelis constant (K_m) values as $-1/(x$ intercepts). Catalysis of the *exo* adduct **17** by 13G5 was characterized in the same manner, and the resulting data were plotted and interpreted in a fashion identical to that shown.

exo Diels–Alder reactions by antibodies 4D5 and 13G5 were examined as random bireactant systems. Both antibodies showed multiple turnovers, and product inhibition was not observed in either case. Double reciprocal Lineweaver–Burk plots were constructed by holding one substrate at a fixed concentration while varying the concentration of the other. From Figure 3, it is seen that for the *endo* Diels–Alderase 4D5, ligand binding (either the diene or dienophile) was completely independent for each substrate within the concentration range studied. A similar pattern was observed for the *exo* Diels–Alderase 13G5. These data provide an accurate estimate of the kinetic parameters of 4D5 or 13G5 either in the presence or absence of the second substrate (Table 1).

Catalytic Antibody Enantioselectivity. We have demonstrated how the enantiomeric pairs of both the *ortho-endo* **16** and *ortho-exo* **17** adducts can be separated by HPLC.[5] The uncatalyzed background reaction (10 mM PBS, pH 7.4, 37 °C) gives a diastereomeric *endo*:*exo* mixture of *ortho* adducts in a ratio of 85:15 as well as the expected 50:50 ratio of each enantiomeric pair.[17]

For this study, antibody catalysis was observed to proceed regioselectively, diastereoselectively (>98% diastereomeric excess), and also enantioselectively. Antibodies 4D5 and 13G5 selectively catalyzed the formation of either a single enantiomer of the *ortho-endo* adduct or a single enantiomer of the *ortho-exo* adduct, respectively, with 95 ± 3% enantiomeric excess.

Enantioselectivity, as viewed from the two subsets of antibody catalysts obtained from haptens **5** and **6**, also merits comment. Structurally the only difference between these haptens is the "linker", and therefore it was not predictable that either hapten would lead to a predominance of *exo* or *endo* antibody catalysts. However, this phenomenon is clearly marked from the data presented (*vide supra*). We suggest the skewing of antibody subset enantioselectivity is due more to "chance" than to any features in the hapten design. Perhaps this is a consequence of our inability to exhaustively screen the complete immune repertoire.

Catalytic Antibody-Hapten Affinity Analysis. An important component of the kinetic analysis of a catalytic antibody is determination of the inhibition constant (K_i) of the hapten. In the present case we were unable to obtain such data because the ferrocenyl inhibitor **18** was susceptible to hydrolysis under our assay conditions.[18] Consequently, antibody-hapten affinity was measured independently by the quenching of intrinsic antibody fluorescence upon binding to a more stable and water soluble ligand. Ferrocene derivative **8** was chosen as a simplified hapten mimic for both antibodies. Compound **8** contains the ferrocene and dimethyl amide functionalities found in both haptens. Titration of **8** with IgG 4D5 or 13G5 followed by Scatchard analysis afforded dissociation constants (K_d) of 209 and 48 μM, respectively.[19] Both antibodies also displayed two binding sites, as expected.

Comparative Analysis of Catalytic Antibodies Generated to Haptens 1 and 2 *versus* 5 and 6: Antibody-Hapten Cross-Reactivity Studies. Having shown that antibody catalysis of the Diels–Alder reaction can be achieved in such a dichotomous manner, using either highly constrained bicyclo[2.2.2]octenes **1** and **2**, or our conformationally flexible ferrocenes **5** and **6** as haptens, we felt it was important to probe the structural requirements of the combining sites of both sets of antibodies. ELISA cross-reactivity studies were undertaken. The results are reported below as the antibody dilution, in parentheses, which was required to give 50% maximum OD at 405 nm. A titer of 256+ was the maximum dilution and hence sensitivity of the assay.

In one experiment, the BSA-**1** and BSA-**2** conjugates were adsorbed onto the surface of 96-well Costar ELISA plates and were allowed to react with the anti-ferrocene antibody catalysts 4D5 (*endo* specificity) and 13G5 (*exo* specificity). The results provided an interesting contrast in cross-reactivity. The *endo* catalyst 4D5 had a reasonably strong preference for the *endo* bicyclo[2.2.2]octene hapten **1** (128+) *versus* the *exo* hapten **2** (8-16). However, the *exo* catalyst 13G5, showed marginal affinity (8-16) for either the *exo* or *endo* haptens. In a second experiment, BSA-**5** and BSA-**6** were affixed to ELISA plates and allowed to react with anti-bicyclo[2.2.2]octene catalytic antibodies, 7D4 (*endo* specificity) and 22C8 (*exo* specificity). In this case both antibodies failed to bind the ferrocenyl haptens to any great extent. These studies, taken as a whole, show that the anti-ferrocene antibody catalysts contain paratopes flexible enough to cross-react with the bicyclo[2.2.2]octene haptens but not *vice versa*. This can be rationalized because of the disparity in the relative size of the two sets of haptens. The ferrocene haptens are much larger, having an inter-ring distance of approximately 3.3 Å, compared to the corresponding 1.55 Å C–C bond-lengths in the bicyclo[2.2.2]octenes.[5] Therefore, it seems reasonable that the ferrocenyl haptens could not enter the binding pockets of the antibodies elicited to the smaller bicyclo[2.2.2]octene haptens. Conversely, the bicyclo[2.2.2]-octene haptens could enter the larger binding pockets of the anti-ferrocenyl antibodies.

The nature of this study and our previous work allows us to make a direct comparison between the two sets of antibodies and the hapten designs which elicited them (Table 1). The Michaelis constant (K_m) was measured for both the diene and dienophile for both sets of antibodies. If we treat these values as representative of apparent dissociation constants for the antibody-substrate complex, then the bicyclo[2.2.2]octene haptens generated marginally tighter antibody-substrate binding complexes than were seen with the ferrocene haptens. To explain this phenomenon, we must look back at the modeling studies of the transition state for this particular reaction, which has been shown to be asynchronous. The C–C bonds being formed have unequal lengths of either 2.05 and 2.35 Å for the

(18) The hydrolysis product of **18** was isolated and characterized by comparing the NMR and mass spectral data to that of the reference compound **11**.

(19) Scatchard, G. *Ann. N.Y. Acad. Sci.* **1949**, *51*, 660.

Table 1. Kinetic Parameters for the Antibody-Catalyzed Diels–Alder Reaction between Diene **3** and Dienophile **4**

hapten	antibody	K_m (diene) (mM)	K_m (dienophile) (mM)	k_{cat} (min^{-1})	k_{uncat} (M^{-1} min^{-1})	k_{cat}/k_{uncat} (M)
1	22C8 (*exo*)	0.70	7.5	3.17×10^{-3}	1.75×10^{-4}	18
2	7D4 (*endo*)	0.96	1.7	3.44×10^{-3}	7.15×10^{-4}	4.8
5	13G5 (*exo*)	2.7	10	1.20×10^{-3}	1.75×10^{-4}	6.9
6	4D5 (*endo*)	1.6	5.9	3.48×10^{-3}	7.15×10^{-4}	4.9

endo transition state or 2.03 and 2.38 Å for the *exo* transition state.[5] For the bicyclo[2.2.2]octene haptens, the relevant C–C bond lengths are 0.5 to 0.85 Å *shorter* than the theorized transition state. In the ferrocenyl haptens, the cyclopentadienyl ring separation is at least 0.90 Å *greater* than in the theorized transition structure, strongly implicating a higher K_m for these antibodies.

In the case of the *exo* catalyst IgG 22C8, this increase in antibody-substrate binding provides only a small increase in k_{cat} compared to IgG 13G5. However, comparison of the two sets of *endo* catalysts, IgG 7D4 and 4D5, shows that this increased antibody-substrate interaction does not manifest any additional advantage in k_{cat}. The "extra" space imparted by the ferrocenyl haptens, while increasing the K_m, may also be serving to increase turnover by allowing the product to diffuse away at a faster rate than it can from the more restricted paratope elicited by the bicyclo[2.2.2]octenes. Thus, it appears that the stereoelectronic features designed into the bicyclo[2.2.2]octene haptens **1** and **2** to model the transition state do not provide any significant advantage over the orbital interactions modeled by the ferrocene immunogens.

Conclusion

In this study we have challenged the dogma that hapten design, for reactions proceeding through a highly-ordered transition-state, must implicitly reflect this highly constrained structure. In contrast, we have found that provided the hapten is able to achieve a conformer which mimics this highly-ordered state, the vast library of the immune system can elicit antibodies to trap this structure and are, therefore, liable to generate catalysts.

From the outset, it was our desire to show that immunization with a single freely-rotating antigen could elicit Diels–Alderases capable of controlling the stereochemical outcome of the reaction. Secondly, we wished to demonstrate that ferrocene can provide an acceptable mimic of the stereoelectronic features important in the transition state of the Diels–Alder reaction. Both concepts were realized during the study, since Diels–Alderases capable of catalyzing the formation of either the *endo* or *exo* adducts were obtained from ferrocene haptens **5** and **6**.

This type of strategy is an alternative to the previously-successful, conformationally-constrained hapten methodology and represents a new application of bioorganometallic chemistry to immunological recognition.[20] Particularly noteworthy of this type of design is that (1) product inhibition concerns identified as a potential problem for antibody-catalyzed Diels–Alder reactions do not occur[4a,c,d] and (2) antibody enhancement of reaction rates, diastereoselectivity, and enantioselectivity are all comparable with those of antibodies elicited from more "classically-designed" haptens for this reaction.

Both haptenic strategies were successful in generating enantioselective Diels–Alderases. However, the rate accelerations seen as a measure of (k_{cat}/k_{uncat}) are still too low to be considered useful for everyday synthetic manipulations. In an attempt to address this problem, new haptens are being designed which will (a) reduce the inter-ring distance so as to approach the "optimal" closer distance for C–C bond formation implicated from theoretical studies and (b) incorporate a Lewis-acid mimic in the ferrocenyl haptens presented here.[21] It is hoped that subsequent studies with antibodies generated to these haptens will highlight more effective catalysts, which retains the exquisite regio- and diastereoselectivity observed in this study.

Perhaps the most exciting feature of our new methodology is its potential generality. The new strategy should not only be applicable to the Diels–Alder cycloaddition but also to other reactions proceeding through highly-ordered, pericyclic, transition states. The only limitation being that the reactions should not face an energy barrier in excess of 20 kcal mol^{-1}, which is widely accepted as being the maximum binding energy an antibody can deliver.

Experimental Section

General Procedures. Unless otherwise stated, reactions were carried out in oven-dried glassware under an atmosphere of nitrogen. Reagents and solvents were transferred with plastic syringes and oven-dried needles.

Dichloromethane and chloroform were continuously distilled from calcium hydride and phosphorus pentoxide, respectively. All reagents were purchased from Aldrich Chemical Company with the exception of *tert*-butyl alcohol which was supplied by Fluka Chemie Ag. All chromatography solvents were obtained commercially and used without further purification.

The R_f values refer to the thin-layer chromatograms developed using 0.25 mm Merck silica gel 60 F-254 glass-supported plates visualized with either ethanolic ninhydrin (1%), phosphomolybdic acid (5%), or an ultraviolet lamp (*N.B.* Ferrocene compounds are colored and can be detected without UV-light). Column chromatography was performed with silica gel 60 (230–400 mesh, E. Merck, Darmstadt, Germany) as described by Still.[22] Yields are for unoptimized procedures and refer to chromatographically and spectroscopically (^{1}H NMR) homogeneous materials, unless otherwise noted.

All proton NMR spectra (300 or 500 MHz) were obtained in CD_3OD, $CDCl_3$, DMSO-d_6 or D_2O at ambient temperature on a Bruker AM-300 or Bruker AMX-500 instrument. ^{13}C NMR spectra were recorded on a Bruker AMX-500 instrument. Chemical shifts (δ) are reported in parts per million relative to internal reference tetramethylsilane and coupling constants (J) are given in Hz. Multiplicities are indicated by s (singlet), d (doublet), t (triplet), q (quartet), qn (quintet), m (multiplet), and br (broad). High and low resolution fast atom bombardment mass spectra were provided by Dr. G. Siudzak of the Scripps Research Institute Mass Spectrometry Facility.

Syntheses of the Haptens, Substrates, and Inhibitors. 1,1′-[(Dimethylamino)carbonyl]ferrocene 8a. *N,N*-Diisopropylethylamine (11.7 mL, 67.2 mmol) was added slowly to a stirred mixture of 1,1′-ferrocenedicarboxylic acid **7** (2.63 g, 9.60 mmol), bis(2-oxo-3-oxazolidinyl)phosphinic chloride (2.44 g, 9.60 mmol), and dimethylamine hydrochloride (3.92 g, 48.0 mmol) in 50 mL of chloroform.

(20) Jaouen, G.; Vessières, A.; Butler, I. S. *Acc. Chem. Res.* **1993**, *26*, 361–369.

(21) (a) Ferricenium hexafluorophosphate has been found to be a weak Lewis acid catalyst of the Diels–Alder reactions between α,β-unsaturated carbonyl compounds and diene. Kelly, T. R.; Maity, S. K.; Meghani, P.; Chandrakumar, N. S. *Tetrahedron Lett.* **1989**, *30*, 1357–1360. (b) Helmchen and co-workers showed that *trans*-(11*R*,12*R*)-bis-(η^5-cyclopentadienylmethyl)dibenzobicyclo[2.2.2]octanoiron(III) tetrafluoroborate catalyzes the Diels–Alder reaction between methacrylaldehyde and cyclopentadiene with high diastereoselectivity: Gibis, K.-L.; Helmchen, G.; Huttner, G.; Zsolnai, L. *J. Organomet. Chem.* **1993**, *445*, 181–186.

(22) Still, W. C.; Kahn, M.; Mitra, A. *J. Org. Chem.* **1978**, *43*, 2923.

(23) Filtration in this stage was used to recover the unreacted 1,1′-ferrocenedicarboxylic acid **7**.

The reaction mixture was then stirred at 0 °C for 1 h. The mixture was acidified with 1 M HCl (20 mL). The organic layer was treated with saturated solution of $NaHCO_3$ (50 mL), washed with CH_2Cl_2 (2 × 100 mL), and dried with $MgSO_4$. Evaporation of the combined CH_2Cl_2 layers gave the neutral bisamide **8a** as a brown-red solid (0.47 g, 15%): ^1H NMR (300 MHz, CD_3OD) δ 3.01 (br s, 3 H), 3.22 (br s, 3 H), 4.46 (br s, 4 H), 4.73 (br s, 4 H); R_f 0.36 (EtOAc/PhMe/HOAc, 5:5:1, PMA); FABLRMS (3-NBA) *m/e* 328 $[M]^+$, 329 $[M + H]^+$.

1-Carboxy-1′-[(dimethylamino)carbonyl]ferrocene 8b. The aqueous layer from the previous reaction was acidified with 1 M HCl (50 mL) and extracted again with CH_2Cl_2 (3 × 100 mL). The combined organic layers were filtered,[23] washed with brine, dried with anhydrous $MgSO_4$, filtered, and evaporated to dryness to afford monoamide **8b** as an orange-red solid (1.68 g, 58%): ^1H NMR (300 MHz, CD_3OD) δ 3.04 (br s, 3 H), 3.25 (br s, 3 H), 4.43 (br s, 2 H), 4.50 (br s, 2 H), 4.72 (br s, 2 H), 4.79 (br s, 2 H); ^{13}C NMR (500 MHz, CD_3OD) δ 37.03, 39.67, 72.61, 72.86, 73.06, 73.51, 74.46, 80.01, 171.9, 174.6); R_f 0.66 (EtOAc/PhMe/HOAc, 5:5:1, PMA); FABLRMS (3-NBA) *m/e* 301 $[M]^+$, 302 $[M + H]^+$; FABLRMS (3-NBA-NaI) *m/e* 324 $[M + Na]^+$; FABHRMS (3-NBA): calcd mass for $C_{14}H_{15}NO_3Fe$ 301.0401, found 301.0389.

1-(Azidocarbonyl)-1′-[(dimethylamino)carbonyl]ferrocene 9. A mixture of **8b** (0.50 g, 1.66 mmol), diphenylphosphoryl azide (0.36 mL, 1.67 mmol), triethylamine (0.96 mL, 3.32 mmol), and toluene (3 mL) was stirred at room temperature for 25 min. The reaction mixture was diluted with 200 mL of CH_2Cl_2, and the organic layer was washed successively with 0.1 M HCl (50 mL), 2 M $NaHCO_3$ (50 mL), and brine (**CAUTION:** The acyl azide is potentially explosive, and the solution should not be evaporated to dryness.). The CH_2Cl_2 layer was dried with anhydrous $MgSO_4$, filtered, and evaporated *in vacuo* to 5 mL to yield acyl azide **9** (0.53 g, 98%): R_f 0.55 (EtOAc/PhMe, 4:1, PMA); FABLRMS (3-NBA) *m/e* 327 $[M + H]^+$.

1-[(Dimethylamino)carbonyl]-1′-[[(1,1-dimethylethoxy)carbonyl]amino]ferrocene 10. The acyl azide **9** (0.53 g, 1.65 mmol) was dissolved in a solution of *tert*-butyl alcohol (20 mL, 0.21 mol) and benzene (5 mL). This mixture was then stirred at 95 °C for 15 min and diluted with CH_2Cl_2 (200 mL). The organic layer was washed with a 5% solution of $NaHCO_3$ (50 mL) and brine. The CH_2Cl_2 layer was dried with $MgSO_4$ and filtered, and the solvent was removed *in vacuo*. The crude residue was chromatographed on silica (EtOAc/PhMe, 1:1) to give carbamate **10** as an orange solid (0.51 g, 83%): ^1H NMR (300 MHz, CD_3OD) δ 2.19 (s, 9 H), 3.02 (br s, 3 H), 3.22 (br s, 3 H), 4.50 (br s, 2 H), 4.63 (br s, 2 H), 4.79 (br s, 2 H), 4.88 (br s, 2 H); R_f 0.48 (EtOAc/PhMe, 1:1, PMA or ninhydrin with 1% trifluoroacetic acid); FABLRMS (3-NBA) *m/e* 372 $[M]^+$, 373 $[M + H]^+$.

1-Amino-1′-[(dimethylamino)carbonyl]ferrocene Hydrochloride 11. A mixture of **10** (0.50 g, 1.34 mmol) and 4 M hydrogen chloride in 1,4-dioxane (3.4 mL, 13.6 mmol) was stirred at room temperature for 20 min. The solvent was removed *in vacuo*, and the residue was lyophilized to afford amine hydrochloride **11** as a deep brown-red solid (0.35 g, 85%): ^1H NMR (300 MHz, DSS D_2O) δ 2.83 (br s, 3 H), 3.06 (br s, 3 H), 4.39 (br s, 2 H), 4.48 (br s, 2 H), 4.73 (br s, 2 H), 4.82 (br s, 2 H); FABLRMS (3-NBA) *m/e* 273 $[M + H]^+$.

1-[(4-Carboxy-1-oxobutyl)amino]-1′-[(dimethylamino)carbonyl]ferrocene 5. A mixture of **11** (0.25 g, 0.81 mmol), glutaric anhydride (0.11 g, 0.96 mmol), and *N,N*-diisopropylethylamine (0.33 mL, 1.89 mmol) was stirred in 10 mL of $CHCl_3$ at 0 °C for 4 h. The reaction mixture was then diluted with dichloromethane (100 mL) and washed with 1 M HCl (20 mL) and brine. The organic layer was dried with anhydrous $MgSO_4$, filtered, and evaporated to dryness. Column chromatography (EtOAc/PhMe/HOAc, 5:5:1) provided carboxylic acid hapten **5** as a red-orange solid (0.28 g, 89%): ^1H NMR (300 MHz, CD_3OD) δ 1.90 (qn, $^3J_{HH}$ = 6.9 Hz, 2 H), 2.25–2.42 (t + t overlapping, 4 H), 3.04 (br s, 3 H), 3.24 (br s, 3 H), 4.49 (br s, 2 H), 4.63 (br s, 2 H), 4.80 (br s, 2 H), 4.87 (br s, 2 H); ^{13}C NMR (500 MHz, CD_3OD) δ 13.80, 21.85, 34.17, 72.98, 73.01, 73.86, 75.60; R_f 0.35 (EtOAc/PhMe/HOAc, 5:5:1, PMA); FABLRMS (3-NBA) *m/e* 387 $[M + H]^+$; FABHRMS (3-NBA-NaI) calcd for $C_{18}H_{22}N_2O_4FeNa$ 409.0827, found 409.0842.

Methyl 4-(Chloroformyl)benzoate 12. A mixture of *mono*-methyl terephthalate (3.00 g, 16.7 mmol) and thionyl chloride (2.4 mL, 32.9 mmol) was refluxed for 4 h. Thionyl chloride was removed *in vacuo* to give acid chloride **12** as a white solid (3.22 g, 97%), which was used without further purification: ^1H NMR (300 MHz, $CDCl_3$) δ 3.98 (s, 3 H), 8.03–8.24 (m, 4 H); FABLRMS (3-NBA) *m/e* 198 $[M]^+$.

1-[(Dimethylamino)carbonyl]-1′-[[4-(methoxycarbonyl)benzoyl]amino]ferrocene 13. A mixture of amine hydrochloride **11** (0.24 g, 0.78 mmol), **12** (0.15 g, 0.76 mmol), and *N,N*-diisopropylethylamine (0.27 mL, 1.55 mmol) in 10 mL of $CHCl_3$ was stirred at 0 °C for 13 h. The reaction mixture was diluted with CH_2Cl_2 (100 mL) and washed with 1 M HCl (30 mL) and brine. The organic layer was dried with anhydrous $MgSO_4$, filtered, and evaporated to dryness. The residue was purified using silica gel chromatography (EtOAc/PhMe, 2:1) to afford **13** as an orange solid (0.30 g, 90%): ^1H NMR (300 MHz, CD_3OD) δ 3.22 (br s, 3 H), 3.43 (br s, 3 H), 3.92 (s, 3 H), 4.13 (m, 2 H), 4.40 (m, 2 H), 4.71 (m, 2 H), 4.79 (m, 2 H), 7.88–8.03 (m, 4 H); R_f 0.36 (EtOAc/PhMe, 2:1); FABLRMS (3-NBA) *m/e* 434 $[M]^+$, 435 $[M + H]^+$.

1-[(4-Carboxybenzoyl)amino]-1′-[(dimethylamino)carbonyl]ferrocene 6. A mixture of **13** (35 mg, 0.081 mmol) and lithium hydroxide monohydrate (10 mg, 0.24 mmol) in 5 mL of MeOH/H_2O (5:1) was stirred at 0 °C for 25 min. The reaction mixture was acidifed with 1 M HCl (5 mL) and extracted with ethyl acetate (3 × 30 mL). The organic layer was washed with brine, dried with anhydrous $MgSO_4$, filtered, and evaporated *in vacuo*. The residue was chromatographed on silica gel (EtOAc/PhMe/HOAc, 5:5:1) to yield hapten **6** as brown-red crystals (31 mg, 91%): ^1H NMR (300 MHz, CD_3OD) δ 2.89 (br s, 3 H), 3.21 (br s, 3 H), 4.18 (m, 2 H), 4.45 (m, 2 H), 4.73 (m, 2 H), 4.80 (m, 2 H), 8.03 (d, $^3J_{HH}$ = 7.6 Hz, 2 H), 8.16 (d, $^3J_{HH}$ = 7.6 Hz, 2 H); R_f 0.25 (EtOAc/PhMe/HOAc, 5:5:1, PMA); FABLRMS (3-NBA) *m/e* 420 $[M]^+$.

4-(Methoxycarbonyl)benzyl *trans*-1,3-Butadiene-1-carbamate 15. A solution of ethyl chloroformate (2.50 g, 23.0 mmol) and 10 mL of acetone was added, over 15 min, to a stirred solution of *trans*-2,4-pentadienoic acid **14** (2.26 g, 23.0 mmol), *N,N*-diisopropylamine (3.68 g, 28.5 mmol), and 20 mL of acetone at 0 °C. After stirring for 45 min at 0 °C, a chilled solution of sodium azide (2.99 g, 46.0 mmol) in 10 mL of water was added. The mixture was stirred for an additional 45 min at 0 °C and poured onto 50 mL of ice water. The acyl azide **19** was isolated by extraction with three 75-mL portions of toluene, dried over $MgSO_4$, filtered, and concentrated to a volume of approximately 150 mL. (**CAUTION:** The acyl azide is potentially explosive. The solution should not be evaporated to dryness.) Methyl 4-(hydroxymethyl)benzoate (3.82 g, 23.0 mmol) in 25 mL of toluene was added to this solution. The reaction mixture was stirred at 100 °C for 40 min, cooled to room temperature, and concentrated to afford a yellow residue, which was purified by silica gel chromatography (EtOAc/hexane 2:1) to afford 3.06 g (51%) of **15** as an off-white crystalline solid: ^1H NMR (500 MHz, DMSO-d_6) δ 9.82 (d, $^3J_{HH}$ = 10.2 Hz, 1 H), 7.96 (d, $^3J_{HH}$ = 8.3 Hz, 2 H), 7.50 (d, $^3J_{HH}$ = 8.2 Hz, 2 H), 6.69 (dd, $^3J_{HH}$ = 10.3 Hz, $^3J_{HH}$ = 13.7 Hz, 1 H), 6.30 (td, $^3J_{HH}$ = 10.6 Hz, $^3J_{HH}$ = 17 Hz, $^3J_{HH}$ = 10.6 Hz, 1 H), 5.75 (dd, $^3J_{HH}$ = 11 Hz, $^3J_{HH}$ = 13.8 Hz, 1 H), 5.18 (s, 2 H), 4.95 (dd, $^3J_{HH}$ = 17 Hz, $^2J_{HH}$ = 1.6 Hz, 1 H), 4.86 (d, $^3J_{HH}$ = 10.1 Hz, $^2J_{HH}$ = 1.5 Hz, 1 H), 3.82 (s, 3 H); R_f 0.75 (EtOAc/hexane 2:1); FABLRMS (3-NBA) *m/e* 261 $[M]^+$; FABLRMS (3-NBA-NaI) *m/e* 284 $[M + Na]^+$.

4-Carboxybenzyl *trans*-1,3-Butadiene-1-carbamate 3. A solution of **15** (1.00 g, 3.83 mmol) and lithium hydroxide monohydrate (0.80 g, 19.2 mmol) in 30 mL of methanol/water (20:1) was stirred for 90 min at 0 °C. The reaction mixture was acidified with 20 mL of 1 M HCl and extracted with ethyl acetate (3 × 150 mL). The combined organic layers were washed with brine (50 mL), dried with $MgSO_4$, and evaporated *in vacuo*. The yellowish residue was purified on silica gel (EtOAc) to give the white product **3** (0.82 g, 87%): ^1H NMR (500 MHz, acetone-d_6) δ 8.83 (br s, 1H), 8.10 (d, $^3J_{HH}$ = 8.0 Hz, 2 H), 7.58 (d, $^3J_{HH}$ = 8.0 Hz, 2 H), 6.85 (dd, $^3J_{HH}$ = 14.5 Hz, 1 H), 6.40 (td, $^3J_{HH}$ = 17 Hz, $^3J_{HH}$ = 10.5 Hz, 1 H), 5.95 (dd, $^3J_{HH}$ = 14 Hz, $^3J_{HH}$ = 11 Hz, 1 H), 5.30 (s, 2 H), 5.04 (dd, $^3J_{HH}$ = 17 Hz, $^2J_{HH}$ = 1.5 Hz, 1 H), 4.89 (dd, $^3J_{HH}$ = 10.5 Hz, $^2J_{HH}$ = 1.5 Hz, 1 H); ^{13}C NMR (500 MHz, DMSO-d_6) δ 65.44, 111.7, 112.4, 127.3, 127.6, 128.6, 129.4, 135.4, 141.4, 153.4, 167.0; FABLRMS (3-NBA) *m/e* 247 $[M]^+$, FABLRMS (3-NBA/NaI) *m/e* 270 $[M + Na]^+$; FABHRMS (3-NBA) calcd for $C_{13}H_{13}NO_4$ 247.0845, found 247.0856.

1-[(Acetyl)amino]-1′-[(dimethylamino)carbonyl]ferrocene 18. Acetyl chloride (14 μL, 0.19 mmol) dissolved in 1 mL of $CHCl_3$ was added dropwise to a stirred solution of **11** (60 mg, 0.19 mmol) and *N,N*-diisopropylethylamine (68 μL, 0.39 mmol) in 2 mL of $CHCl_3$ at 0 °C. The reaction mixture was stirred at room temperature for 2 h and extracted with 2 × 50 mL of ethyl acetate. The combined organic layers were washed with brine, dried with anhydrous $MgSO_4$, filtered, and evaporated *in vacuo*. The residue was chromatographed on silica gel (PhMe/EtOAc, 1:1) to yield inhibitor **18** as dark red crystals (56 mg, 91%): ^{1}H NMR (300 MHz, CD_3OD) δ 1.94 (s, 3 H), 3.05 (br s, 3 H), 3.25 (br s, 3 H), 4.49 (m, 2 H), 4.63 (m, 2 H), 4.81 (m, 2 H), 4.89 (m, 2 H); ^{13}C NMR (500 MHz, CD_3OD) δ 32.11, 39.25, 42.11, 72.98, 73.01, 73.86, 75.60, 79.80, 83.20, 170.2, 171.9); R_f 0.35 (PhMe/EtOAc 1:1, UV, PMA); FABLRMS (3-NBA) *m/e* 315 $[M + H]^+$; FABHRMS (3-NBA) calcd for $C_{15}H_{18}N_2O_2FeNa$ 337.0615, found 337.0629.

Hapten-Carrier Protein Conjugation. Activated hapten solutions were prepared by adding 1.3 mol equiv of 1-(3-dimethylaminopropyl)-3-ethylcarbodiimide hydrochloride (EDC) and *N*-hydroxysulfosuccinimide (Sulfo-NHS) in water to a solution of haptens **5** and **6** (4 mg) in DMF (200 μL). After a 24 h incubation at room temperature, the keyhole limpet hemocyanin (KLH) conjugates were prepared by adding 100 μL of the activated hapten solution to a solution of 5 mg of KLH in 900 μL of 50 mM PBS (pH 7.5). The bovine serum albumin (BSA) conjugates were prepared similarly. The hapten-protein conjugates were incubated at 4 °C for 24 h.

HPLC Kinetic Studies. A solution of antibody in 10 mM PBS, pH 7.4 at 37 °C was assayed with substrates **3** and **4** in the same buffer to give a final solution containing 20 μM of antibody 4D5 or 13G5, 0.67 to 8 mM of diene, and 1 to 8 mM of dienophile. HPLC assays were performed on a VYDAC 201TP54 C_{18} reverse-phase column with an isocratic program of 85% water (0.1% trifluoroacetic acid) and 15% acetonitrile flowing at 2.0 mL/min. Product formation was quantitated against an internal standard (80 μM, *N*-propyl-2-methylbenzamide), at a wavelength of 240 nm. The retention times of the *endo* (t_R = 13.0 min) and *exo* (t_R = 11.1 min) adducts formed in the catalyzed reactions were identical with those of authentic samples of synthesized **16** and **17**.

HPLC Studies for Determining Enantiomeric Excess. We have reported earlier[5] that the four enantiomeric *ortho* adducts (two *exo* and two *endo*) could be simultaneously separated by HPLC using a normal-phase DAICEL Chiralpak AD column with an isocratic mobile phase of 70% hexane (1.5% trifluoroacetic acid) and 30% isopropyl alcohol flowing at 1 mL/min, λ = 240 nm. In our hands, the retention times of the two *exo* adducts were 6.5 and 7.7 min, while the *endo* adducts eluted at 8.8 and 10.7 min. Unfortunately, under these conditions the substrate diene **3** has a retention time of 7.0 min meaning it coelutes with the *exo* adducts. It is, therefore, necessary to separate the enantiomers from reaction mixtures containing any excess diene prior to their injection onto the chiral column.

For our assays we typically set up 1 mL reactions containing 20 μM mAb 13G5 or 4D5 and 4−8 mM diene and dienophile substrates which were allowed to incubate for 3−7 days at 37 °C. We then isolated the formed enantiomeric adducts (together) by injecting the reaction mixtures onto a reverse-phase semipreparative HPLC column (VYDAC 201TP510) and eluting with 85% water (0.1% trifluoroacetic acid) and 15% acetonitrile at 6 mL/min, λ = 240 nm. Retention times for the *exo* adducts, *endo* adducts, and diene on the semipreparative column were 14.0, 16.0, and 52.0 min, respectively. The mobile phase was removed by a combination of rotary evaporation and high vacuum pump. The *exo/endo* adducts were then redissolved in a small volume (100 μL) of equimixture CH_2Cl_2/MeOH/*n*-hexanes, and aliquots were injected onto the analytical chiral column. Individual enantiomer concentrations from antibody-catalyzed reactions were compared with those from appropriate controls in order to determine relative enantiomeric excesses. Interestingly, antibodies 13G5 and 4D5 selectively catalyzed formation of the same *exo* and *endo* enantiomers as antibodies 22C8 and 7D4 reported previously.[5]

Fluorescence Quench Experiments. Antibodies were diluted to 0.1 μM in a final volume of 2 mL with 5% DMF in 10 mM PBS, pH 7.4. Fluorescence was measured on an SLM Aminco SPF5000C spectrofluorometer with excitation and emission wavelength at 280 and 338 nm, respectively. The solution of **8** prepared in 5% DMF and 10 mM PBS, pH 7.4 was added sequentially to the antibody solution. The background fluorescence quench was measured by adding 5% DMF in 10 mM PBS, pH 7.4 into the same antibody solution. The bound antibody was determined as the percentage of quench $(Q_0/Q_{max}) \times$ [mAb], where Q_0 is the measured decrease from the initial fluorescence, and Q_{max} was experimentally determined as 90 at high concentrations of **8**. Estimates of average intrinsic affinity were calculated from a Scatchard plot.

Catalytic Antibody Cross-Reactivity Studies. Each well of a Costar 96-well microtiter plate was precoated with 25 μL of the primary antigen (BSA-**1**, **2**, **5**, **6**; 5 mg/mL each conjugate) at 1:1000 dilution. The plate was dried overnight at 37 °C, and on day two the wells were fixed with 50 μL/well methanol and allowed to incubate for 5 min at 25 °C. Methanol was removed, and the plate was allowed to air dry for 10 min. To prevent nonspecific adsorption, 50 μL/well of BLOTTO was added to the wells. After incubating for 5 min, the BLOTTO was shaken out, and 25 μL/well of new BLOTTO was added to facilitate titering. A 25 μL sample of each catalytic antibody was added to each of the designated wells and serially diluted across the plate. The plate was incubated at 37 °C for 1 h in a moist chamber and then washed 20 times with deionized water. Next, 25 μL of a 1:1000 dilution of a goat anti-mouse IgG, glucose-oxidase conjugate (Cappel) was added to each well, and the plate was incubated at 37 °C for a further 1 h in a moist chamber. The plate was again washed 20 times with deionized water, and bound antibody was detected with the addition of 50 μL of developing agent (0.6 μL 20% glucose, 40 μL ABTS, 40 μL HRPO in 5 mL of phosphate buffer pH 6.0) to each well. Thirty minutes later the plate absorbance was read at 405 nm.

Acknowledgment. This work was supported by TEKES, Technology Development Centre, The Finnish Centre for International Mobility and Exchange Programmes, Helsinki, Finland, The A. P. Sloan Foundation, and National Science Foundation. We thank Diane Kubitz for her expert assistance with antibody production and Dr. Paul Wentworth and Dr. Donald Hilvert for helpful comments. Dr. Veronique Gouverneur is acknowledged for providing the sample of cycloadducts **16** and **17** and Marika Aaltokari for valuable help with the synthesis of the inhibitors.

JA950341Q